Percolation transition in quantum Ising and rotor models with sub-Ohmic dissipation

Manal Al-Ali,[1] José A. Hoyos,[2] and Thomas Vojta[1]
[1]*Department of Physics, Missouri University of Science and Technology, Rolla, Missouri 65409, USA*
[2]*Instituto de Física de São Carlos, Universidade de São Paulo, C.P. 369, São Carlos, São Paulo 13560-970, Brazil*
(Received 28 June 2012; published 13 August 2012)

We investigate the influence of sub-Ohmic dissipation on randomly diluted quantum Ising and rotor models. The dissipation causes the quantum dynamics of sufficiently large percolation clusters to freeze completely. As a result, the zero-temperature quantum phase transition across the lattice percolation threshold separates an unusual super-paramagnetic cluster phase from an inhomogeneous ferromagnetic phase. We determine the low-temperature thermodynamic behavior in both phases, which is dominated by large frozen and slowly fluctuating percolation clusters. We relate our results to the smeared transition scenario for disordered quantum phase transitions, and we compare the cases of sub-Ohmic, Ohmic, and super-Ohmic dissipation.

DOI: 10.1103/PhysRevB.86.075119 PACS number(s): 75.10.Nr, 75.40.−s, 05.30.Rt, 64.60.Bd

I. INTRODUCTION

The interplay between geometric, quantum, and thermal fluctuations in randomly diluted quantum many-particle systems leads to a host of unconventional low-temperature phenomena. These include the singular thermodynamic and transport properties in quantum Griffiths phases[1,2] as well as the exotic scaling behavior of the quantum phase transitions between different ground state phases.[3,4] Recent reviews of this topic can be found, e.g., in Refs. 5 and 6.

An especially interesting situation arises if a quantum many-particle system is diluted beyond the percolation threshold p_c of the underlying lattice (see, e.g., Ref. 7 and references therein). Although the resulting percolation quantum phase transition is driven by the geometric fluctuations of the lattice, the quantum fluctuations lead to critical behavior different from that of classical percolation. In the case of a diluted transverse-field Ising magnet, the transition displays exotic activated (exponential) dynamic scaling[8] similar to what is observed at infinite-randomness critical points.[3,4] The percolation transition of the quantum rotor model shows conventional scaling (at least in the particle-hole symmetric case where topological Berry phase terms are unimportant[9]), but with critical exponents that differ from their classical counterparts.[10,11] For site-diluted Heisenberg quantum antiferromagnets, further modifications of the critical behavior were attributed to uncompensated geometric Berry phases.[12,13]

In many realistic systems, the relevant degrees of freedom are coupled to an environment of "heat-bath" modes. The resulting dissipation can qualitatively change the low-energy properties of a quantum many-particle system. In particular, it has been shown that dissipation can further enhance the effects of randomness on quantum phase transitions. In generic random quantum Ising models, for instance, the presence of Ohmic dissipation completely destroys the sharp quantum phase transition by smearing[14–19] while it leads to infinite-randomness critical behavior in systems with continuous-symmetry order parameter.[20–22] Interestingly, super-Ohmic dissipation does not change the universality class of random quantum Ising models[17,19] but plays a major role in systems with continuous-symmetry order parameter.[23]

It is therefore interesting to ask what are the effects of dissipation on randomly diluted quantum many-particle systems close to the percolation threshold. It has recently been shown that Ohmic dissipation in a diluted quantum Ising model leads to an unusual percolation quantum phase transition[24] at which some observables show classical critical behavior while others are modified by quantum fluctuations.

In the present paper, we focus on the influence of sub-Ohmic dissipation (which is qualitatively stronger than the more common Ohmic dissipation) on diluted quantum Ising models and quantum rotor models. When coupled to a sub-Ohmic bath, even a single quantum spin displays a nontrivial quantum phase transition from a fluctuating to a localized phase[25] whose properties have attracted considerable attention recently (see, e.g., Ref. 26 and references therein). Accordingly, we find that the quantum dynamics of sufficiently large percolation clusters freezes completely as a result of the coupling to the sub-Ohmic bath, effectively turning them into classical moments. The interplay between large frozen clusters and smaller dynamic clusters gives rise to unconventional properties of the percolation transition, which we explore in detail.

Our paper is organized as follows: In Sec. II, we define our models and discuss their phase diagrams at a qualitative level. Section III is devoted to a detailed analysis of the quantum rotor model in the large-N limit where all calculations can be performed explicitly. In Sec. IV, we go beyond the large-N limit and develop a general scaling approach. We conclude in Sec. V.

II. MODELS AND PHASE DIAGRAMS

A. Diluted dissipative quantum Ising and rotor models

We consider two models. The first model is a d-dimensional ($d \geqslant 2$) site-diluted transverse-field Ising model[8,27–29] given by the Hamiltonian

$$H_I = -J \sum_{\langle i,j \rangle} \eta_i \eta_j \sigma_i^z \sigma_j^z - h_x \sum_i \eta_i \sigma_i^x, \qquad (1)$$

a prototypical disordered quantum magnet. The Pauli matrices σ_i^z and σ_i^x represent the spin components at site i, the exchange interaction J couples nearest neighbor sites, and the transverse field h_x controls the quantum fluctuations. Dilution is introduced via the random variables η_i which can take the values 0 and 1 with probabilities p and $1-p$, respectively.

We now couple each spin to a local heat bath of harmonic oscillators,[16,30]

$$H = H_I + \sum_{i,n} \eta_i \left[\nu_{i,n} a^\dagger_{i,n} a_{i,n} + \frac{1}{2} \lambda_{i,n} \sigma^z_i (a^\dagger_{i,n} + a_{i,n}) \right], \quad (2)$$

where $a_{i,n}$ ($a^\dagger_{i,n}$) is the annihilation (creation) operator of the nth oscillator coupled to spin i, $\nu_{i,n}$ is its natural frequency, and $\lambda_{i,n}$ is the coupling constant. All baths have the same spectral function

$$\mathcal{E}(\omega) = \pi \sum_n \lambda^2_{i,n} \delta(\omega - \nu_{i,n}) = 2\pi\alpha\omega_c^{1-\zeta}\omega^\zeta e^{-\omega/\omega_c}, \quad (3)$$

with α and ω_c being the dimensionless dissipation strength and the cutoff energy, respectively. The exponent ζ characterizes the type of dissipation; we are mostly interested in the sub-Ohmic case $0 < \zeta < 1$. For comparison, we will also consider the Ohmic ($\zeta = 1$) and super-Ohmic cases ($\zeta > 1$). Experimentally, local dissipation (with various spectral densities) can be realized, e.g., in molecular magnets weakly coupled to nuclear spins[31,32] or in magnetic nanoparticles in an insulating host.[33]

The second model is a site-diluted dissipative quantum rotor model which can be conveniently defined in terms of the effective Euclidean (imaginary time) action[10]

$$\begin{aligned} \mathcal{A} &= \int d\tau \sum_{\langle ij \rangle} J \eta_i \eta_j \boldsymbol{\phi}_i(\tau) \cdot \boldsymbol{\phi}_j(\tau) + \sum_i \eta_i \mathcal{A}_{\rm dyn}[\boldsymbol{\phi}_i] \\ \mathcal{A}_{\rm dyn}[\boldsymbol{\phi}] &= \frac{\alpha}{2} T \sum_{\omega_n} \omega_c^{1-\zeta} |\omega_n|^\zeta \tilde{\boldsymbol{\phi}}(\omega_n) \cdot \tilde{\boldsymbol{\phi}}(-\omega_n). \end{aligned} \quad (4)$$

Here, the random variables $\eta_i = 0,1$ again implement the site dilution, and ω_n are bosonic Matsubara frequencies. The rotor at site i and imaginary time τ is described by $\boldsymbol{\phi}_i(\tau)$: a N-component vector of length $N^{1/2}$. Its Fourier transform in imaginary time is denoted by $\tilde{\boldsymbol{\phi}}(\omega_n)$. The dynamic action $\mathcal{A}_{\rm dyn}$ stems from integrating out the heat-bath modes, with the parameter α measuring the strength of the dissipation, and the exponent ζ characterizing the type of the dissipation, as in the first model [see Eq. (3)].

B. Classical percolation theory

We now briefly summarize the results of percolation theory[34] to the extent necessary for our purposes. Consider a regular d-dimensional lattice in which each site is removed at random with probability p.[35] For small p, the resulting diluted lattice is still connected in the sense that there is a cluster of connected nearest neighbor sites (called the percolating cluster) that spans the entire system. For large p, on the other hand, a percolating cluster does not exist. Instead, the lattice is made up of many isolated clusters consisting of just a few sites.

In the thermodynamic limit of infinite system volume, the two regimes are separated by a sharp geometric phase transition at the percolation threshold $p = p_c$. The behavior of the lattice close to p_c can be understood as a geometric critical phenomenon. The order parameter is the probability P_∞ of a site to belong to the infinite connected percolation cluster. It is obviously zero in the disconnected phase ($p > p_c$) and nonzero in the percolating phase ($p < p_c$). Close to p_c, it varies as

$$P_\infty \sim |p - p_c|^{\beta_c} \quad (p < p_c), \quad (5)$$

where β_c is the order parameter critical exponent of classical percolation. (We use a subscript c to distinguish quantities associated with the lattice percolation transition from those of the quantum phase transitions discussed below). In addition to the infinite cluster, we also need to characterize the finite clusters on both sides of the percolation threshold. Their typical size, the correlation or connectedness length ξ_c, diverges as

$$\xi_c \sim |p - p_c|^{-\nu_c} \quad (6)$$

with ν_c the correlation length exponent. The average mass S_c (number of sites) of a finite cluster diverges with the susceptibility exponent γ_c according to

$$S_c \sim |p - p_c|^{-\gamma_c}. \quad (7)$$

The complete information about the percolation critical behavior is contained in the cluster size distribution n_s, i.e., the number of clusters with s sites excluding the infinite cluster (normalized by the total number of lattice sites). Close to the percolation threshold, it obeys the scaling form

$$n_s(p) = s^{-\tau_c} f[(p - p_c)s^{\sigma_c}]. \quad (8)$$

Here, τ_c and σ_c are critical exponents. The scaling function $f(x)$ is analytic for small x and has a single maximum at some $x_{\rm max} > 0$. For large $|x|$, it drops off rapidly:

$$f(x) \sim \exp(-B_1 x^{1/\sigma_c}) \quad (x > 0), \quad (9)$$

$$f(x) \sim \exp[-(B_2 x^{1/\sigma_c})^{1-1/d}] \quad (x < 0), \quad (10)$$

where B_1 and B_2 are constants of order unity. The classical percolation exponents are determined by τ_c and σ_c: the correlation lengths exponent $\nu_c = (\tau_c - 1)/(d\sigma_c)$, the order parameter exponent $\beta_c = (\tau_c - 2)/\sigma_c$, and the susceptibility exponent $\gamma_c = (3 - \tau_c)/\sigma_c$. Right at the percolation threshold, the cluster size distribution does not contain a characteristic scale, $n_s \sim s^{-\tau_c}$, yielding a fractal critical percolation cluster of fractal dimension $D_f = d/(\tau_c - 1)$.

C. Phase diagrams

Let us now discuss in a qualitative fashion the phase diagrams of the models introduced in Sec. II A, beginning with the diluted dissipative quantum Ising model Eq. (2). If we fix the bath parameters ζ and ω_c and measure all energies in terms of the exchange interaction J, we still need to explore the phases in the three-dimensional parameter space of transverse field h_x, dissipation strength α and dilution p. A sketch of the phase diagram is shown in Fig. 1. For sufficiently large transverse field and/or sufficiently weak dissipation, the ground state is paramagnetic for all values of the dilution p. This is the conventional paramagnetic phase that can be found for $h_x > h_\infty(\alpha)$ or, correspondingly, for $\alpha < \alpha_\infty(h_x)$. Here, $h_\infty(\alpha)$ is the transverse field at which the undiluted bulk system undergoes the transition at fixed α while $\alpha_\infty(h_x)$ is its critical dissipation strength at fixed h_x.

The behavior for $h_x < h_\infty(\alpha)$ [or $\alpha > \alpha_\infty(h_x)$] depends on the dilution p. It is clear that magnetic long-range order

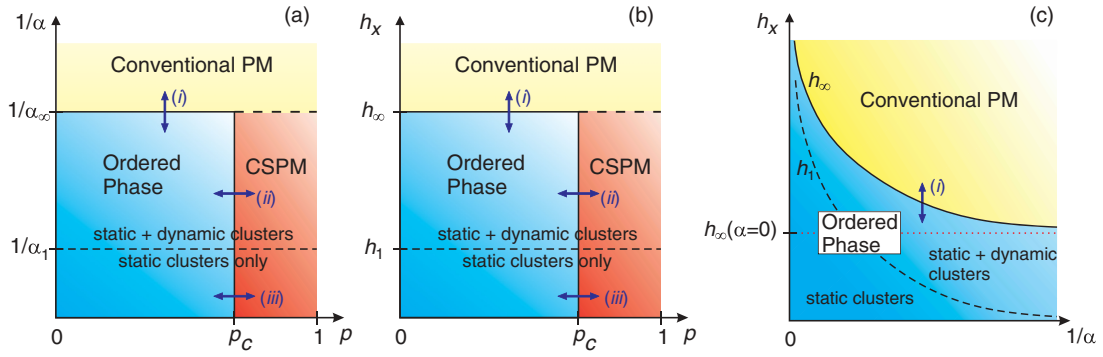

FIG. 1. (Color online) Schematic ground state phase diagram of the diluted dissipative quantum Ising model [Eq. (2)] for fixed values of $\zeta < 1$, ω_c, and J. The three panels show three cuts through the three-dimensional parameter space of dilution p, transverse field h_x, and dissipation strength α. (a) α-p phase diagram at a fixed transverse field h_x with $h_x > h_\infty$ ($\alpha = 0$) such that the dissipationless system is in the paramagnetic phase. This phase diagram also applies to the rotor model Eq. (4). (b) h_x-p phase diagram at a fixed dissipation strength α. (c) h_x-α phase diagram at fixed dilution $p < p_c$. CSPM refers to the cluster super-paramagnetic phase, transition (i) denotes the smeared generic (field or dissipation-driven) quantum phase transition, and (ii) and (iii) denote the percolation quantum phase transitions in the two regimes with or without dynamic clusters, respectively.

is impossible for $p > p_c$, because the lattice consists of finite-size clusters that are completely decoupled from each other. Each of these clusters acts as an independent magnetic moment. For $h_x < h_\infty(\alpha)$ and $p > p_c$, the system is thus in a cluster super-paramagnetic phase.

Let us consider a single cluster of s sites in more detail. For small transverse fields, its low-energy physics is equivalent to that of a sub-Ohmic spin-boson model, i.e., a single effective Ising spin (whose moment is proportional to s) in an effective transverse-field $h_x(s) \sim h_x e^{-Bs}$ with $B \sim \ln(J/h_x)$ and coupled to a sub-Ohmic bath with an effective dissipation strength $\alpha_s = s\alpha$.[8,24] With increasing dissipation strength and/or decreasing transverse field, this sub-Ohmic spin-boson model undergoes a quantum phase transition from a fluctuating to a localized (frozen) ground state.[25] This implies that sufficiently large percolation clusters are in the localized phase, i.e., they behave as classical moments. The cluster super-paramagnetic phase thus consists of two regimes. If the transverse field is not too small, $h_1(\alpha) < h_x < h_\infty(\alpha)$ [or if the dissipation is not too strong, $\alpha_1(h_x) > \alpha > \alpha_\infty(h_x)$], static and dynamic clusters coexist. Here, $h_1(\alpha)$ is the critical field of a *single* spin in a bath of dissipation strength α while $\alpha_1(h_x)$ is its critical dissipation strength in a given field h_x. In contrast, for $h_x < h_1(\alpha)$ [or $\alpha > \alpha_1(h_x)$] all clusters are frozen, and the system behaves purely classically.

Finally, for dilutions $p < p_c$, there is an infinite-spanning percolation cluster that can support magnetic long-range order. Naively, one might expect that the critical transverse-field (at fixed dissipation strength α) decreases with dilution p because the spins are missing neighbors. However, in our case of sub-Ohmic dissipation, rare vacancy-free spatial regions can undergo the quantum phase transition independently from the bulk system. As a consequence, the field-driven transition [transition (i) in Fig. 1] is smeared,[15,18] and the ordered phase extends all the way to the clean critical field $h_\infty(\alpha)$ for all $p < p_c$. Analogous arguments apply to the critical dissipation strength at fixed transverse field h_x.

The infinite percolation cluster coexists with a spectrum of isolated finite-size clusters whose behavior depends on the transverse field and dissipation strength. Analogous to the super-paramagnetic phase discussed above, the ordered phase thus consists of two regimes. For $h_1(\alpha) < h_x < h_\infty(\alpha)$ [or $\alpha_1(h_x) > \alpha > \alpha_\infty(h_x)$], static (frozen) and dynamic clusters coexist with the long-range-ordered infinite cluster. For $h_x < h_1(\alpha)$ [or $\alpha > \alpha_1(h_x)$], all clusters are frozen, and the system behaves classically.

The phase diagram of the diluted quantum rotor model with sub-Ohmic dissipation (4) can be discussed along the same lines. After fixing the bath parameters ζ and ω_c and measuring all energies in terms of the exchange interaction J, we are left with two parameters, the dilution p and the dissipation strength α. The zero-temperature behavior of a single quantum rotor coupled to a sub-Ohmic bath is analogous to that of the corresponding quantum Ising spin. With increasing dissipation strength, the rotor undergoes a quantum phase transition from a fluctuating to a localized ground state. This follows, for instance, from mapping[36] the sub-Ohmic quantum rotor model onto a one-dimensional classical Heisenberg chain with an interaction that falls off more slowly than $1/r^2$. This model is known to have an ordered phase for sufficiently strong interactions.[37] As a result, all the arguments used above to discuss the phase diagram of the diluted sub-Ohmic transverse-field Ising model carry over to the rotor model [Eq. (4)]. The α-p phase diagram of the rotor model thus agrees with the phase diagram shown in Fig. 1(a).

In the following sections, we investigate the percolation quantum phase transitions of the models Eqs. (2) and (4), i.e., the transitions occurring when the dilution p is tuned through the lattice percolation threshold p_c. These transitions are marked in Fig. 1 by (ii) and (iii).

III. DILUTED QUANTUM ROTOR MODEL IN THE LARGE-N LIMIT

In this section, we focus on the diluted dissipative quantum rotor model in the large-N limit of an infinite number of order-parameter components. In this limit, the problem turns into a

self-consistent Gaussian model. Consequently, all calculations can be performed explicitly.

A. Single percolation cluster

We begin by considering a single percolation cluster of s sites. For $\alpha > \alpha_\infty$, this cluster is locally in the ordered phase. Following Refs. 38 and 39, it can therefore be described as a single large-N rotor with moment s coupled to a sub-Ohmic dissipative bath of strength $\alpha_s = s\alpha$. Its effective action is given by

$$\mathcal{A}_{\text{eff}} = T\sum_{\omega_n}\left[\frac{1}{2}\tilde{\psi}(\omega_n)\Gamma_n\tilde{\psi}(-\omega_n) - s\tilde{H}_z(\omega_n)\tilde{\psi}(-\omega_n)\right], \quad (11)$$

where $\Gamma_n = \epsilon + s\alpha\omega_c^{1-\zeta}|\omega_n|^\zeta$, ψ represents one rotor component, and H_z is an external field conjugate to the order parameter.

In the large-N limit, the renormalized distance ϵ from criticality of the cluster is fixed by the large-N (spherical) constraint $\langle|\psi(\tau)|^2\rangle = 1$. In terms of the Fourier transform, $\tilde{\psi}(\omega_n)$ defined by

$$\psi(\tau) = T\sum_{\omega_n}\tilde{\psi}(\omega_n)\exp[-i\omega_n\tau], \quad (12)$$

the large-N constraint for a constant field H_z becomes

$$T\sum_{\omega_n}\frac{1}{\epsilon + s\alpha\omega_c^{1-\zeta}|\omega_n|^\zeta} + \left(\frac{sH_z}{\epsilon}\right)^2 = 1. \quad (13)$$

Solving this equation gives the renormalized distance from criticality ϵ as a function of the cluster size s.

At zero temperature and field, the sum over the Matsubara frequencies turns into an integration, and the constraint equation reads

$$\frac{1}{\pi}\int_0^{\omega_c} d\omega \frac{1}{\epsilon_0 + s\alpha\omega_c^{1-\zeta}|\omega|^\zeta} = 1. \quad (14)$$

(We denote the renormalized distance from criticality at zero temperature and field by ϵ_0.) The critical size s_c above which the cluster freezes can be found by setting $\epsilon_0 = 0$ and performing the integral (14). This gives

$$s_c = 1/[\pi\alpha(1-\zeta)]. \quad (15)$$

As we are interested in the critical behavior of the clusters, we now solve the constraint equation for cluster sizes close to the critical one, $s_c - s \ll s_c$. This can be accomplished by subtracting the constraints at s and s_c from each other. We need to distinguish two cases: $1/2 < \zeta < 1$ and $\zeta < 1/2$. In the first case, the resulting integral can be easily evaluated after moving the cutoff ω_c to infinity. This gives

$$\epsilon_0 = \alpha s_c[-\zeta\sin(\pi/\zeta)\alpha(s_c - s)]^{\zeta/(1-\zeta)}\omega_c \quad (\text{for } \zeta > 1/2). \quad (16)$$

In the second case, $\zeta < 1/2$, we can evaluate Eq. (14) via a straight Taylor expansion in $(s_c - s)$. This results in

$$\epsilon_0 = \alpha^2 s_c\pi(1-2\zeta)(s_c - s)\omega_c \quad (\text{for } \zeta < 1/2). \quad (17)$$

It will be useful to rewrite Eqs. (16) and (17) in a more compact manner:

$$\epsilon_0(s) = [A_\zeta(1 - s/s_c)]^{x/(1-x)}\omega_c, \quad (18)$$

where $A_\zeta = -(\alpha s_c)^{1/\zeta}\zeta\sin(\pi/\zeta)$ for $\zeta > 1/2$, and $A_\zeta = (\alpha s_c)^2\pi(1-2\zeta)$ for $\zeta < 1/2$, and $x = \max\{1/2, \zeta\}$.

In order to compute thermodynamic quantities, we will also need the value of $\epsilon(s)$ at nonzero temperature. The constraint equation for small but nonzero temperature can be obtained by keeping the $\omega_n = 0$ term in the frequency sum of Eq. (13) discrete, while representing all other modes in terms of an ω integral. This gives

$$\frac{T}{\epsilon} + \frac{1}{\pi}\int_0^{\omega_c} d\omega \frac{1}{\epsilon + s\alpha\omega_c^{1-\zeta}|\omega|^\zeta} = 1. \quad (19)$$

Solving this equation for asymptotically low temperatures results in the following behaviors. For clusters larger than the critical size, $s > s_c$, ϵ vanishes linearly with T via $\epsilon = Ts/(s - s_c)$. Clusters of exactly the critical size have $\epsilon = A_\zeta^x\omega_c^{1-x}T^x$. For smaller clusters ($s < s_c$), low temperatures only lead to a small correction of the zero-temperature behavior ϵ_0. Writing $\epsilon(T) = \epsilon_0 + \delta T$, we obtain $\delta = [s/(s_c - s)][x/(1-x)]$. Clusters with sizes close to the critical one show a crossover from the off-critical to the critical regime with increasing T. For $s \lesssim s_c$, this means

$$\epsilon(T) \approx \begin{cases}\epsilon_0(1 + \delta T/\epsilon_0) & (\text{for } \epsilon_0 \gg \epsilon_T),\\ \epsilon_T & (\text{otherwise}),\end{cases} \quad (20)$$

with $\epsilon_T = A_\zeta^x\omega_c^{1-x}T^x$.

The constraint equation at zero temperature but in a nonzero ordering field H_z can be solved analogously.[39] For asymptotically small fields, we find $\epsilon(H_z) = sH_z[s/(s - s_c)]^{1/2}$ in the case of clusters of size $s > s_c$. At the critical size, $\epsilon(H_z) = [A_\zeta^x\omega_c^{1-x}(s_cH_z)^{2x}]^{1/(1+x)}$, and for $s < s_c$ we obtain $\epsilon(H_z) = \epsilon_0 + \delta(sH_z)^2/\epsilon_0$. Larger fields lead to a crossover from the off-critical to the critical regime. For $s \lesssim s_c$, it reads

$$\epsilon(H_z) \approx \begin{cases}\epsilon_0[1 + \delta(sH_z/\epsilon_0)^2] & (\text{for } \epsilon_0 \gg \epsilon_{H_z}),\\ \epsilon_{H_z} & (\text{otherwise}),\end{cases} \quad (21)$$

with $\epsilon_{H_z} = [A_\zeta^x\omega_c^{1-x}(sH_z)^{2x}]^{1/(1+x)}$.

Observables of a single cluster can now be determined by taking the appropriate derivatives of the free energy $F_{cl} = -T\ln(Z)$ with

$$Z = \prod_n Z_n, \quad (22)$$

where

$$Z_n = \frac{T}{\epsilon + s\alpha\omega_c^{1-\zeta}|\omega_n|^\zeta}\exp\left(\frac{T}{2}\frac{s\tilde{H}_z(\omega_n)s\tilde{H}_z(-\omega_n)}{\epsilon + s\alpha\omega_c^{1-\zeta}|\omega_n|^\zeta}\right). \quad (23)$$

The dynamical (Matsubara) susceptibility and magnetization are then given by

$$\chi_{cl}(i\omega_n) = \frac{s^2}{\epsilon + s\alpha\omega_c^{1-\zeta}|\omega_n|^\zeta}, \quad (24)$$

and

$$m_{cl}(\omega_n) = T\frac{s^2\tilde{H}_z(\omega_n)}{\epsilon + s\alpha\omega_c^{1-\zeta}|\omega_n|^\zeta}, \quad (25)$$

respectively, where ϵ is given by the solution of the constraint equation discussed above. (Note that the contribution of a cluster of size s to the uniform susceptibility is proportional to s^2). Therefore, in the above two limiting cases, we can write

the uniform and static susceptibility of a cluster of size $s < s_c$ as a function of temperature as follows:

$$\chi_{cl}(T) \approx s^2/\epsilon(T). \tag{26}$$

Large clusters ($s > s_c$) behave classically, $\chi_{cl} \approx s(s - s_c)/T$, at low temperatures. Finally, for the critical ones $\chi_{cl} \approx s^2/\epsilon_T$.

In order to calculate the retarded susceptibility $\chi_{cl}(\omega)$, we need to analytically continue the Matsubara susceptibility by performing a Wick rotation to real frequency, $i\omega_n \to \omega + i0$. The resulting dynamical susceptibility reads

$$\chi_{cl}(\omega) = \frac{s^2}{\epsilon + \alpha\omega_c^{1-\zeta}|\omega|^\zeta[\cos(\pi\zeta/2) - i\,\sin(\pi\zeta/2)\mathrm{sgn}(\omega)]}. \tag{27}$$

Using Eq. (21), the single cluster magnetization in a small ordering constant field H_z is given by

$$m_{cl} = \chi_{cl}H_z \approx \begin{cases} H_z s^2/\epsilon_0 & (\text{for } \epsilon_0 \gg \epsilon_{H_z}), \\ H_z s^2/\epsilon_{H_z} & (\text{otherwise}). \end{cases} \tag{28}$$

Thermal properties (at zero field) can be computed by using the "remarkable formulas" derived by Ford *et al.*,[40] which express the free energy (the internal energy) of a quantum oscillator in a heat bath in terms of its susceptibility and the free energy (internal energy) of the free oscillator. For our model, they read, respectively

$$F_{cl} = -\mu + \frac{1}{\pi}\int_0^\infty \mathrm{d}\omega F_f(\omega,T)\mathrm{Im}\left[\frac{d}{d\omega}\ln\chi_{cl}(\omega)\right], \tag{29}$$

and

$$U_{cl} = -\mu + \frac{1}{\pi}\int_0^\infty \mathrm{d}\omega U_f(\omega,T)\mathrm{Im}\left[\frac{d}{d\omega}\ln\chi_{cl}(\omega)\right]. \tag{30}$$

Here, $F_f(\omega,T) = T\ln[2\sinh(\omega/(2T))]$ and $U_f(\omega,T) = (\omega/2)\coth(\omega/(2T))$. The extra μ terms stem from the Lagrange multiplier enforcing the large-N constraint.[39]

The entropy $S_{cl} = (U_{cl} - F_{cl})/T$ can be calculated simply by inserting Eq. (27) into Eqs. (29) and (30) and computing the resulting integral. For the dynamical clusters ($s < s_c$), the low-temperature entropy behaves as

$$S_{cl} = B_\zeta \alpha s \omega_c^{1-\zeta}\frac{T^\zeta}{\epsilon_0}, \tag{31}$$

where B_ζ is a ζ-dependent constant. At higher temperatures (greater than $T^* \sim \epsilon_0^{1/\zeta}\omega_c^{1-1/\zeta}$), the entropy becomes weakly dependent on T.[41]

In the low-T limit, the specific heat $C_{cl} = T(\partial S_{cl}/\partial T)$ thus behaves as

$$C_{cl} = B_\zeta \zeta \alpha s \omega_c^{1-\zeta}\frac{T^\zeta}{\epsilon_0}. \tag{32}$$

B. Complete system

After discussing the behavior of a single percolation cluster, we now turn to the full diluted lattice model. The low-energy density of states of the dynamic clusters $\rho_{dy}(\epsilon) = \sum_{s<s_c} n_s\delta(\epsilon - \epsilon_0(s))$ is obtained combining the single-cluster result [Eq. (18)] with the cluster-size distribution [Eq. (8)], yielding

$$\rho_{dy}(\epsilon) = A_\zeta^{-1}(x^{-1} - 1)\frac{n_{s(\epsilon)}s_c}{\omega_c}\left(\frac{\epsilon}{\omega_c}\right)^{(1-2x)/x}, \tag{33}$$

where $s(\epsilon)$ is the size of a cluster with renormalized distance ϵ from criticality [which can be obtained inverting Eq. (18)]. Notice that ρ_{dy} shows no dependence on ϵ in the case $\zeta < 1/2$. In particular, it does not diverge with $\epsilon \to 0$, in contrast to the case $\zeta > 1/2$.

We now discuss the physics at the percolation transition, starting with the total magnetization m. We have to distinguish the contributions m_{dy} from dynamical clusters, m_{st} from frozen finite-size clusters, and m_∞ from the infinite percolation cluster, if any. For zero ordering field H_z, m_{dy} vanishes, because the dynamic clusters fluctuate between up and down. The frozen finite-size clusters individually have a nonzero magnetization, but it sums up to zero ($m_{st} = 0$), because they do not align coherently for $H_z = 0$. Hence, the only coherent contribution to the total magnetization is m_∞. Since the infinite cluster is long-range ordered for small transverse field $h_x < h_\infty(\alpha)$, its magnetization is proportional to the number P_∞ of sites in the infinite cluster, giving

$$m = m_\infty \sim P_\infty(p) \sim \begin{cases} |p - p_c|^{\beta_c} & (\text{for } p < p_c), \\ 0 & (\text{for } p > p_c). \end{cases} \tag{34}$$

The magnetization critical exponent β is therefore given by its classical lattice percolation value β_c. In response to an infinitesimally small ordering field H_z, the frozen finite-size clusters align at zero temperature, leading to a jump in $m(H_z)$ at $H_z = 0$. The magnitude of the jump is given by $m_{st} = \sum_{s>s_c} n_s$. At the percolation threshold, $m_{st} \approx (1 - p_c)s_c^{2-\tau_c}$, and it vanishes exponentially for both $p \to 0$ and $p \to 1$. The total magnetization in an infinitesimal field (given by $m_\infty + m_{st}$) is analytic at $p = p_c$, and only clusters with sizes below s_c are not polarized.

To estimate the contribution m_{dy} of the dynamic clusters, we integrate the magnetization of a single cluster [Eq. (28)] over the DOS given in Eq. (33). For $\zeta > 1/2$, we find that

$$m_{dy} = C_\zeta n_{s_c} s_c^2\left(\frac{H_z s_c}{\omega_c}\right)^{3(1-\zeta)/(1+\zeta)}, \tag{35}$$

where n_{s_c} is the density of critical clusters, and $C_\zeta = A_\zeta^{-3\zeta/(1+\zeta)}\zeta/(2\zeta - 1)$. For $\zeta < 1/2$, the integration gives

$$m_{dy} = \frac{n_{s_c}s_c^2}{A_\zeta}\left(\frac{s_c H_z}{\omega_c}\right)\left[1 + \ln\left(\frac{\theta_0}{\left(A_\zeta\omega_c s_c^2 H_z^2\right)^{1/3}}\right)\right], \tag{36}$$

where θ_0 is a cutoff energy.

Because the three contributions to the magnetization have different field dependence, the system shows unconventional hysteresis effects. The infinite cluster has a regular hysteresis loop (for $p < p_c$), the finite-size frozen clusters do not show hysteresis, but they contribute jumps in $m(H_z)$ at $H_z = 0$, and the dynamic clusters contribute a continuous but singular term (see Fig. 2).

The low-temperature susceptibility is dominated by the contribution χ_{st} of the static clusters, with each one adding a Curie term of the form $s(s - s_c)/T$. Summing over all static

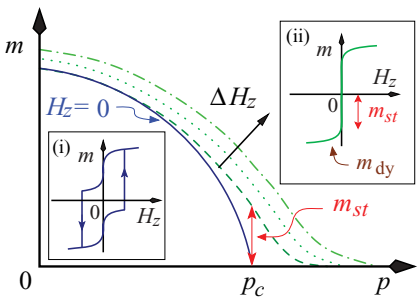

FIG. 2. (Color online) The magnetization as a function of dilution p for different ordering fields H_z at absolute zero. The solid line is the magnetization at $H_z = 0$ (the contribution of the infinite cluster only). The dashed line is for an infinitesimal field, and the remaining ones represent stronger fields. Insets display the hysterisis curves in the (i) ordered and (ii) disordered phases.

clusters, close to the percolation threshold, we find that

$$\chi_{st} \sim \sum_{s>s_c} n_s \frac{s(s-s_c)}{T} \sim \frac{1}{T}|p-p_c|^{-\gamma_c}. \tag{37}$$

For $p \to 0$ and $p \to 1$, the prefactor of the Curie term vanishes exponentially. The infinite cluster contribution χ_∞ remains finite (per site) for $T \to 0$, because the infinite cluster is in the ordered phase.

To determine the contribution χ_{dy} of the dynamical clusters, we integrate the single-cluster susceptibility [Eq. (26)] over the low-energy DOS in Eq. (33). For $\zeta > 1/2$, this gives

$$\chi_{dy} = C'_\zeta \frac{n_{s_c} s_c^3}{\omega_c} \left(\frac{T}{\omega_c}\right)^{1-2\zeta}, \tag{38}$$

with $C'_\zeta = A_\zeta^{-2\zeta}[\zeta/(2\zeta-1)]$. For $\zeta < 1/2$, we find

$$\chi_{dy} = A_\zeta^{-1} \frac{n_{s_c} s_c^3}{\omega_c} \left[1 + \ln\left(\frac{\theta_0}{(A_\zeta \omega_c T)^{1/2}}\right)\right]. \tag{39}$$

The retarded susceptibility of the fluctuating clusters can be obtained by integrating the single-cluster susceptibility [Eq. (27)] over the distribution [Eq. (33)]. This leads to

$$\mathrm{Im}\,\chi_{dy}(\omega) = D_\zeta \frac{n_{s_c} s_c^3}{\omega_c} \left|\frac{\omega}{\omega_c}\right|^{1-2x} \mathrm{sgn}(\omega), \tag{40}$$

with $D_\zeta = A_\zeta^{-1}(\frac{1}{x}-1)\pi \sin(\theta(\frac{1}{x}-2))/[\sin(\frac{\pi}{x})(\pi(1-\zeta))^{\frac{1}{x}-2}]$. We notice that Im χ_{dy} has no ω dependence for $\zeta < 1/2$.

Finally, we consider the heat capacity. The dynamical cluster contribution can be obtained by summing the single-cluster heat capacity [Eq. (32)] over $\rho_{dy}(\epsilon)$, yielding $C_{dy} \sim n_{s_c} s_c (T/\omega_c)^{1-\zeta}$ for $\zeta > 1/2$ and $C_{dy} \sim n_{s_c} s_c (T/\omega_c)^{\zeta}$ for $\zeta < 1/2$.

IV. BEYOND THE LARGE-N LIMIT: SCALING APPROACH

In the last subsection, we have studied the percolation quantum phase transition of the diluted sub-Ohmic rotor model [Eq. (4)] in the large-N limit. Let us now go beyond the large-N limit and consider the rotor model with a finite number of components as well as the quantum Ising model [Eq. (2)].

We begin by analyzing a single percolation cluster of s sites. For strong dissipation $\alpha > \alpha_\infty$ (or weak fluctuations $h_x < h_\infty$), this cluster can be treated as a compact object that fluctuates in (imaginary) time only. As pointed out in Sec. II C, in the presence of sub-Ohmic dissipation, such a cluster undergoes a continuous quantum phase transition from a fluctuating to a localized phase as a function of increasing dissipation strength or, equivalently, cluster size s.

Even though the critical behavior of this quantum phase transition is not exactly solvable, we can still write down a scaling description of the cluster free energy

$$F_{cl}(r, H_z, T) = b^{-1} F_{cl}(r b^{1/(\nu_s z_s)}, H_z b^{y_s}, T b), \tag{41}$$

where $r = \alpha_s - \alpha_c = (s - s_c)\alpha$ is the distance from criticality, b is an arbitrary scale factor, and $\nu_s z_s$ and y_s are the critical exponents of the single-cluster quantum phase transition. (We use a subscript s to distinguish the single-cluster exponents from those associated with the percolation quantum phase transition of the diluted lattice.)

Normally, one would expect the two exponents $\nu_s z_s$ and y_s to be independent. However, because the sub-Ohmic damping corresponds to a long-range interaction in time, the exponent η takes the mean-field value $2 - \zeta$ for all ζ.[42–44] This also fixes the exponent y_s in Eq. (41) to be $y_s = (1 + \zeta)/2$. Thus, there is only one independent exponent in addition to ζ; in the following we choose the susceptibility exponent γ_s. This implies, via the usual scaling relations, that the correlation time exponent is given by $\nu_s z_s = \gamma_s/\zeta$.

The values of the cluster exponents in the large-N case of Sec. III are given by $\gamma_s = \zeta/(1-\zeta)$ and $\nu_s z_s = 1/(1-\zeta)$. In the general case of finite-N rotors and for the quantum Ising model, they can be found numerically. Notice the scaling form of the free energy [Eq. (41)] applies to bath exponents $\zeta > 1/2$. For $\zeta < 1/2$, the single-cluster critical behavior is mean-field-like.

The behavior of single-cluster observables close to the (single-cluster) quantum critical point can now be obtained by taking the appropriate derivatives of the free energy [Eq. (41)]. For example, the static magnetic susceptibility at $T = 0$ and $H_z = 0$ behaves as

$$\chi(r, \omega = 0) \sim r^{-\gamma_s}. \tag{42}$$

Using this result, we can derive a generalization of the probability distribution $\rho_{dy}(\epsilon)$ of the inverse static susceptibilities $\epsilon = \chi^{-1}$. We find

$$\rho_{dy}(\epsilon) = \int_1^{s_c} \mathrm{d}s\, n_s\, \delta[\epsilon - c(s_c - s)^{\gamma_s}] \sim n_{s_c}\, \epsilon^{(1-\gamma_s)/\gamma_s} \tag{43}$$

right at the percolation threshold. In the large-N limit, $\gamma_s = \zeta/(1-\zeta)$ implying $\rho_{dy}(\epsilon) \sim \epsilon^{(1-2\zeta)/\zeta}$ in agreement with the explicit result in Eq. (33).

Let us now discuss how the properties of the percolation quantum phase transition in the general case differ from those obtained in the large-N limit in Sec. III B. We focus on the case $\zeta > 1/2$. If the single-cluster critical behavior is of mean-field type ($\zeta < 1/2$), the functional forms of the results in Sec. III B are not modified at all. The total magnetization is the sum of the magnetization m_∞ of the infinite percolation cluster, m_{st} stemming from the large ($s > s_c$) frozen percolation clusters, and m_{dy} provided by the dynamic clusters having $s < s_c$. Both m_∞ and m_{st} are completely independent of the single-cluster critical behavior. The behavior of the spontaneous (zero-field)

magnetization across the percolation transition in the general case is thus identical to that of the large-N limit [see Eq. (34) and Fig. 2]. In contrast, the magnetization–magnetic field curve of the dynamic clusters does depend on the value of γ_s. Integrating the single cluster magnetization of all dynamic clusters [analogous to Eq. (28)] gives

$$m_{dy} \sim H_z^{[1-\zeta+2\zeta/\gamma_s]/(1+\zeta)}. \tag{44}$$

In the large-N limit, this recovers the result [Eq. (35)], as expected.

The low-temperature susceptibility can be discussed along the same lines. The contributions χ_∞ and χ_{st} do not depend on the single-cluster critical behavior. Integrating the single-cluster susceptibility over all dynamic clusters using (43) yields (at $p = p_c$)

$$\chi_{dy} \sim T^{(1-\gamma_s)\zeta/\gamma_s}. \tag{45}$$

If we use the large-N value of γ_s, we reproduce Eq. (38).

The scaling ansatz [Eq. (41)] for the single-cluster free energy thus allows us to discuss the complete thermodynamics across the percolation quantum phase transition. Dynamic quantities can be analyzed in the same manner. For example, the scaling form of the single-cluster dynamic susceptibility reads

$$\chi_{cl}(r, H_z, T, \omega) = b^{2y_s-1}\chi_{cl}(rb^{1/(\nu_s z_s)}, H_z b^{y_s}, Tb, \omega b). \tag{46}$$

The contribution of the fluctuating clusters to the low-temperature dynamic susceptibility can be found by integrating the single-cluster contribution over the distribution [Eq. (43)]. This leads to

$$\mathrm{Im}\,\chi_{dy}(\omega) \sim |\omega|^{(1-\gamma_s)\zeta/\gamma_s}\,\mathrm{sgn}(\omega). \tag{47}$$

In the large-N limit this corresponds to $\mathrm{Im}\,\chi_{dy}(\omega) \sim |\omega|^{1-2\zeta}\,\mathrm{sgn}(\omega)$ in agreement with Eq. (40) for $\zeta > 1/2$. In summary, even though the critical behavior is not exactly solvable for finite-N rotors and quantum Ising models, we can express the properties of the percolation quantum phase transition in terms of a single independent exponent of the single-cluster problem (which can be found, e.g., numerically).

V. CONCLUSIONS

We have investigated the effects of local sub-Ohmic dissipation on the quantum phase transition across the lattice percolation threshold of diluted quantum Ising and rotor models. Experimentally, such local dissipation (with various spectral densities) can be realized, e.g., in molecular magnets weakly coupled to nuclear spins[31,32] or in magnetic nanoparticles in an insulating host.[33] Further potential applications include diluted two-level atoms in optical lattices coupled to an electromagnetic field, random arrays of tunneling impurities in crystalline solids or, in the future, large sets of coupled qubits in noisy environments.

As even a single spin or rotor undergoes a localization quantum phase transition for sufficiently strong sub-Ohmic damping, the quantum dynamics of large percolation clusters in the diluted lattice freezes completely. The coexistence of these frozen clusters which effectively behave as classical magnetic moments and smaller fluctuating clusters, if any, leads to unusual properties of the percolation quantum phase transition. In this final section, we put our results into broader perspective.

Let us compare the three different quantum phase transitions separating the paramagnetic and ferromagnetic phases [transitions (i), (ii), and (iii) in Fig. 1]. The generic transition (i) occurs as a function of transverse field or dissipation strength for $p < p_c$. This transition is smeared by the mechanism of Ref. 15 because rare vacancy-free spatial regions can undergo the quantum phase transition independently from the bulk system. For $p < p_c$, these rare regions are weakly coupled leading to magnetic long-range order instead of a quantum Griffiths phase.[18,19]

In contrast, the percolation transitions (ii) and (iii) are not smeared but sharp. The reason is that different percolation clusters are completely decoupled for $p > p_c$. Thus, even if some of these clusters have undergone the (localization) quantum phase transition and display local order, their local magnetizations do not align, leading to an incoherent contribution to the global magnetization. Deviations from a pure percolation scenario change this conclusion. If the interaction has long-range tails (even very weak ones), different frozen clusters will be coupled, and their magnetizations align coherently. This leads to a smearing of the dilution-driven transition analogous to that of the transition (i). However, if the long-range tail of the interaction is weak, the effects of the smearing become important at the lowest energies only. What is the difference between the percolation transitions (ii) and (iii) in Fig. 1? If all percolation clusters are frozen [transitions (iii)] low-temperature observables behave purely classically. If large frozen and smaller dynamic clusters coexist [transitions (ii)] quantum fluctuations contribute to the observables at the percolation transition.

We now compare the case of sub-Ohmic dissipation considered here to the cases of Ohmic and super-Ohmic dissipation as well as the dissipationless case. To do so, we need to distinguish the quantum Ising model and the rotor model.

The percolation transitions of the dissipationless and super-Ohmic rotor models display conventional critical behavior, but with critical exponents that differ from the classical percolation exponents.[38] (This holds for the particle-hole symmetric case in which complex Berry phase terms are absent from the action.[9]) In the Ohmic rotor model, the percolation transition displays activated scaling as at infinite-randomness critical points.[38]

For the diluted quantum Ising model, the percolation transition displays activated scaling already in the dissipationless[8] and super-Ohmic cases.[19] In the presence of Ohmic dissipation, sufficiently large percolation clusters can undergo the localization transition independently from the bulk. The resulting percolation transition[24] is similar to the one discussed in the present paper; it shows unusual properties due to an interplay of frozen and dynamic percolation clusters.

All these results suggest that quantum phase transitions across the lattice percolation threshold can be classified analogously to generic disordered phase transitions[5,10] (provided the order parameter action does not contain complex terms). If a single finite-size percolation cluster is below the lower critical dimension of the problem, it can not undergo a phase transition independent of the bulk system. The resulting percolation

transition displays conventional critical behavior (this is the case for the dissipationless and super-Ohmic rotor models). If a single finite-size cluster can undergo the transition by itself (i.e., it is above the lower critical dimension of the problem), the resulting percolation transition is unconventional with some observables behaving classically while others are influenced by quantum fluctuations. This scenario applies to the sub-Ohmic models studied in this paper as well as the Ohmic quantum Ising model. Finally, if a single percolation cluster is right at the lower critical dimension (but does not undergo a phase transition), the percolation quantum phase transition shows activated critical behavior. This scenario applies to the dissipationless quantum Ising model as well as the Ohmic quantum rotor model.

ACKNOWLEDGMENTS

This work has been supported in part by the NSF under Grant No. DMR-0906566, by FAPESP under Grant No. 2010/03749-4, and by CNPq under Grant Nos. 590093/2011-8 and 302301/2009-7.

[1] M. Thill and D. A. Huse, Physica A **214**, 321 (1995).
[2] A. P. Young and H. Rieger, Phys. Rev. B **53**, 8486 (1996).
[3] D. S. Fisher, Phys. Rev. Lett. **69**, 534 (1992).
[4] D. S. Fisher, Phys. Rev. B **51**, 6411 (1995).
[5] T. Vojta, J. Phys. A **39**, 143R (2006).
[6] T. Vojta, J. Low Temp. Phys. **161**, 299 (2010).
[7] T. Vojta and J. A. Hoyos, in *Recent Progress in Many-Body Theories*, edited by J. Boronat, G. Astrakharchik, and F. Mazzanti (World Scientific, Singapore, 2008), p. 235.
[8] T. Senthil and S. Sachdev, Phys. Rev. Lett. **77**, 5292 (1996).
[9] R. M. Fernandes and J. Schmalian, Phys. Rev. Lett. **106**, 067004 (2011).
[10] T. Vojta and J. Schmalian, Phys. Rev. B **72**, 045438 (2005).
[11] T. Vojta and R. Sknepnek, Phys. Rev. B **74**, 094415 (2006).
[12] L. Wang and A. W. Sandvik, Phys. Rev. Lett. **97**, 117204 (2006).
[13] L. Wang and A. W. Sandvik, Phys. Rev. B **81**, 054417 (2010).
[14] A. J. Millis, D. K. Morr, and J. Schmalian, Phys. Rev. Lett. **87**, 167202 (2001).
[15] T. Vojta, Phys. Rev. Lett. **90**, 107202 (2003).
[16] G. Schehr and H. Rieger, Phys. Rev. Lett. **96**, 227201 (2006).
[17] G. Schehr and H. Rieger, J. Stat. Mech. (2008) P04012.
[18] J. A. Hoyos and T. Vojta, Phys. Rev. Lett. **100**, 240601 (2008).
[19] J. A. Hoyos and T. Vojta, Phys. Rev. B **85**, 174403 (2012).
[20] J. A. Hoyos, C. Kotabage, and T. Vojta, Phys. Rev. Lett. **99**, 230601 (2007).
[21] A. Del Maestro, B. Rosenow, M. Müller, and S. Sachdev, Phys. Rev. Lett. **101**, 035701 (2008).
[22] T. Vojta, C. Kotabage, and J. A. Hoyos, Phys. Rev. B **79**, 024401 (2009).
[23] T. Vojta, J. A. Hoyos, P. Mohan, and R. Narayanan, J. Phys.: Condens. Matter **23**, 094206 (2011).
[24] J. A. Hoyos and T. Vojta, Phys. Rev. B **74**, 140401(R) (2006).
[25] R. Bulla, N.-H. Tong, and M. Vojta, Phys. Rev. Lett. **91**, 170601 (2003).
[26] A. Winter, H. Rieger, M. Vojta, and R. Bulla, Phys. Rev. Lett. **102**, 030601 (2009).
[27] A. B. Harris, J. Phys. C **7**, 3082 (1974).
[28] R. Stinchcombe, J. Phys. C **14**, L263 (1981).
[29] R. R. dos Santos, J. Phys. C **15**, 3141 (1982).
[30] L. F. Cugliandolo, G. S. Lozano, and H. Lozza, Phys. Rev. B **71**, 224421 (2005).
[31] N. V. Prokofev and P. C. E. Stamp, Rep. Prog. Phys. **63**, 669 (2000).
[32] I. Chiorescu, W. Wernsdorfer, A. Müller, H. Bögge, and B. Barbara, Phys. Rev. Lett. **84**, 3454 (2000).
[33] W. Wernsdorfer, Adv. Chem. Phys. **118**, 99 (2001).
[34] D. Stauffer and A. Aharony, *Introduction to Percolation Theory* (CRC Press, Boca Raton, 1991).
[35] In agreement with Sec. II A, we define p as the fraction of sites removed rather than the fraction of sites present.
[36] S. Sachdev, *Quantum phase transitions* (Cambridge University Press, Cambridge, 1999).
[37] J. Fröhlich, R. Israel, E. H. Lieb, and B. Simon, Commun. Math. Phys. **62**, 1 (1978).
[38] T. Vojta and J. Schmalian, Phys. Rev. Lett. **95**, 237206 (2005).
[39] M. Al-Ali and T. Vojta, Phys. Rev. B **84**, 195136 (2011).
[40] G. W. Ford, J. T. Lewis, and R. F. O'Connell, Ann. Phys. (NY) **185**, 270 (1988).
[41] For $\zeta < 1/2$ it has a logarithmic T dependence, while for $\zeta > 1/2$ its dependence on T is even weaker (Ref. 39).
[42] M. E. Fisher, S.-K. Ma, and B. G. Nickel, Phys. Rev. Lett. **29**, 917 (1972).
[43] J. Sak, Phys. Rev. B **15**, 4344 (1977).
[44] E. Luijten and H. W. J. Blöte, Phys. Rev. Lett. **89**, 025703 (2002).